Accepted Manuscript

New Organocobaloxime Derivatives – Synthesis, Characterization, Catalase-like Activity and DFT Studies

Mukadder Erdem-Tunçmen, Fatma Karipcin, Murat Atiş, Sabriye Perçin-Özkorucuklu

PII: S0022-328X(14)00038-2

DOI: 10.1016/j.jorganchem.2014.01.023

Reference: JOM 18464

To appear in: *Journal of Organometallic Chemistry*

Received Date: 6 September 2013

Revised Date: 14 January 2014

Accepted Date: 18 January 2014

Please cite this article as: M. Erdem-Tunçmen, F. Karipcin, M. Atiş, S. Perçin-Özkorucuklu, New Organocobaloxime Derivatives – Synthesis, Characterization, Catalase-like Activity and DFT Studies, *Journal of Organometallic Chemistry* (2014), doi: 10.1016/j.jorganchem.2014.01.023.

Two new organocobaloxime derivatives synthesized and characterized by elemental, thermal analysis, FT-IR, ^{1}H NMR, magnetic susceptibility measurements, cyclic voltammetry and DFT calculations. The experimental and theoretical chemical shift results are generally in good agreement. Synthesized compounds were also evaluated for their catecholase-like activity.

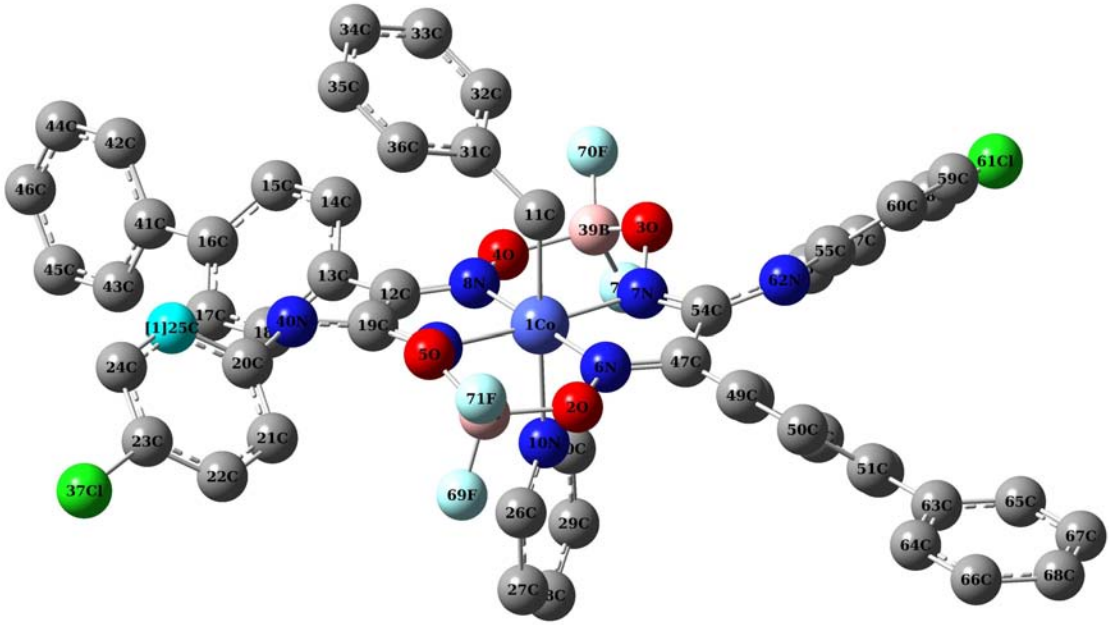

New Organocobaloxime Derivatives – Synthesis, Characterization, Catalase-like Activity and DFT Studies

Mukadder Erdem-Tunçmen[a], Fatma Karipcin[b*], Murat Atiş[c], Sabriye Perçin-Özkorucuklu[a]

[a]*Department of Chemistry, Sciences and Arts Faculty, Süleyman Demirel University, 32260, Isparta-TURKEY*

[b]*Department of Chemistry, Sciences and Arts Faculty, Nevsehir Hacı Bektaş Veli University, 50300, Nevsehir-TURKEY*

[c]*Kayseri Vocational School, Erciyes University, 38039 Melikgazi, Kayseri-TURKEY*

**Tel: +90 384 2153900 Fax: +90 384 2153948 E-mail: fkaripcin@nevsehir.edu.tr*

Abstract

New organocobaloxime derivatives of the types $[Co(HL)_2(Bz)Py]$ and $[CoL_2(Bz)PyB_2F_4]$ [H_2L = 4-(4-chlorophenylamino)biphenylglyoxime; Bz = Benzyl; Py = Pyridine] were synthesized and characterized by elemental analysis, molar conductance, FT-IR, ^1H NMR and magnetic susceptibility measurements. The structural and vibrational spectroscopic data of the molecule in the ground state were calculated by the density functional method using the 6-31G(d) basis set. Isotropic chemical shifts (^1H and ^{13}C NMR) were calculated using the gauge-invariant atomic orbital (GIAO) method. In addition, the thermal decomposition of complexes with H_2L was studied in nitrogen atmosphere. The IR spectra indicated that the complexes coordinate through the N atom of the oxime group of the ligand. The diamagnetic susceptibilities of the complexes indicated that they are diamagnetic (low-spin d^6 octahedral). The catalase-like activities of the complexes for the disproportionation of hydrogen peroxide were investigated in the presence of imidazole. The redox behaviors of the ligand and its complexes were investigated by cyclic voltammetry at the platinum electrode in DMF.

Keywords: Organocobaloximes, BF_2^+ bridged, catalase-like activity, CV, DFT, B3LYP

1. Introduction

The chemistry of oxime/oximato metal complexes has been investigated actively since the time of the first synthesis, e.g. preparation of nickel(II) dimethylglyoximate, and recognition of the chelate five-membered character of this complex by Tschugaeff [1] and has been reviewed in several studies [2-5]. Oximes and their metal complexes are of current interest for their rich physicochemical properties, reactivity patterns and potential applications in many important chemical processes in the areas of medicine, bioorganic systems, catalysis, electrochemical and electrooptical sensors [6].

Vitamin B_{12} is one of the naturally occurring coordination compounds in biology. The active component of liver extract was first separated and finally crystallized in 1948 [7, 8]. In 1965, Dorothy Hodgkin determined the structure crystallographically. The successful determination of the molecular structure of coenzyme B_{12} provided an unexpected surprise in that it contained an apparently stable carbon–cobalt bond. This is the only naturally occurring organometallic compound. An intriguing aspect of the B_{12} system is the great stability of the carbon–cobalt bond. Although the alkyl–cobalt bond in alkyl cobalamins is surprisingly stable, it can be cleaved and transferred into a number of other chemical species. The organometallic chemistry of cobalt in vitamin B_{12} and its derivatives is unusual and interesting. The most commonly mentioned B_{12} model system is the bis(dimethylglyoximato)cobalt complex. These complexes are often referred to as cobaloximes. The common feature of the different models is that each possesses a very strong equatorial ligand field [8].

The organocobaloximes $RCo(DH)_2L$, where R = alkyl group, DH = monoanion of dimethylglyoxime and L = neutral ligand, were synthesized at the beginning of the 1960s [9].

The immediately became the subject of extensive studies, because they were considered as good models of vitamin B_{12} [10-27].

In this paper, we report on the synthesis, characterization and thermal stabilities of a series of cobalt(III) glyoximato complexes using the dioxime ligand [4-(4-chlorophenylamino)biphenylglyoxime], axial base (py) and benzyl as alkyl. Additionally we prepared BF_2^+-bridge containing complexes by replacing the bridging protons of the cobalt(III)–dioxime complex with the BF_2 group. Particularly significant in this work is the inclusion of the BF_2 bridge group, which we anticipated would generate some unique structural diversity. We also report the results of the calculated structure, the vibrational and NMR spectra of the title molecules, the calculations being made on the basis of the density functional theory (DFT) approximations. In a subsequent paper, we will be reporting studies on the use of organocobaloxime analogues as models of vitamin B_{12}.

2. Results and discussion

2.1. Synthesis

The ligand [4-(4-chlorophenylamino)biphenylglyoxime](Fig. 1) was obtained by the reaction of p-chloroaniline with 4-biphenylchloroglyoxime in the presence of triethylamine. The product, a yellow powder material, was characterized by IR, ^{1}H NMR spectroscopy and elemental analyses. Attempts to isolate crystals of the complexes suitable for X-ray diffraction were unsuccessful. Therefore, elemental analysis, spectroscopic techniques, conductivity and magnetic susceptibility techniques were employed in order to determine the structural characteristics of the complexes. The analytical and physical data for the ligand and its complexes are in good agreement with expected values.

The molar conductance of the complexes was an aid for their proposed formulas. The conductivity measurements of the complexes were determined using freshly prepared

solutions of the complexes in DMF at room temperature. The values of the molar conductance in DMF in 10^{-3} mol L^{-1} solutions are 20 and 30 Ω^{-1} cm^2 mol^{-1}, suggesting a non-electrolytic nature for mononuclear complexes (respectively 1, 2) [28,29].

The magnetic susceptibility measurements of the complexes were carried out in the solid state at room temperature and provided information regarding their structures. The magnetic susceptibility measurements showed that the mononuclear cobalt complexes (**1, 2**) are diamagnetic, which corresponds to the +3 oxidation state of cobalt (low spin octahedral d^6-system, S = 0).

2.2. IR Spectra

The observed IR spectra of the free ligand and its complexes exhibit various bands in the 400–4000 cm^{-1} region. The theoretical wavenumbers along with their relative intensities are given as Supporting Information in Tables S1-S3. Because there was no imaginary frequency for the stationary points, the optimized structures were accepted as real minimums. To bring the theoretical values closer to the experimental values, we used two different scaling factors, i.e. 0.983 up to 1700 cm^{-1} and 0.958 for greater than 1700 cm^{-1} [30]. The observed IR spectrum of the dioxime ligand showed a υ(C=N) peak at 1596 and 1635 cm^{-1} and a υ(N-O) peak at 1092 cm^{-1}, as reported for similar ligands [31–33]. The appearances of two bands for the C=N groups indicate the asymmetrical nature of the free ligands. The appropriate calculated frequencies of υ(C=N) are positioned at 1520 and 1634 cm^{-1} and υ(N-O) is positioned at 1093 cm^{-1}, when the DFT/B3LYP/6-31G(d) method was applied.

The bands are assigned to the υ(C=N) stretching frequency shift to 1575 and 1590–1592 cm^{-1} in the complexes. These bands are shifted to lower wavenumbers in the complexes. Burger et al. [34] reported, on the basis of the frequency shift of the C=N vibrations that the lower the C=N vibration frequency, the stronger the metal → N=C donor π-bond. The results

suggest that the increase in electron density on the cobalt causes the increase of back donation from cobalt to the nitrogen atoms of the dioxime ligands, resulting in the increase in conjugation of the five-membered chelate rings. The same vibrations appear in the theoretical calculation at 1591-1554 and 1615-1620 cm^{-1}. Similar trends have been reported in the literature for cobaloxime derivatives [33, 34]. The υ(N–O) stretching frequencies shift to 1011-1091 cm^{-1} in the complexes and their corresponding calculated wavenumbers appeared at 1096 and 1094 cm^{-1}.

The coordination of the axial electron donating base to the Co atom causes an increase in electron density in the Co atom. This facilitates the back donation from Co to the nitrogen atoms of the dioxime ligands, resulting in an increase in electron densities in the C=N and N–O bonds. The increase in electron density in N–O bonds causes stronger hydrogen bridges of O–H…O and the higher frequency shifts of N–O stretching vibrations. The facilitated back donation from cobalt to the nitrogen atoms of the dioxime ligand results in increased metal-donor π-bond in the equatorial moiety of cobaloximes, which causes the stronger interaction of Co with equatorial N atoms and brings about conjugation in the five-membered chelate rings including Co atom, resulting in lower frequency shift of the υ(C=N) vibrations [33, 35, 36]. The spectra of all the complexes exhibit a new band at around 500 cm^{-1} (498 and 515 cm^{-1}) which is not found in the spectrum of free ligand. In agreement with IR spectral studies on cobaloximes this band is assigned to Co–N stretching frequency between Co and the nitrogen atoms of the dioxime ligands. We assigned a band due to the Co–N stretching based on the TED calculations, and obtained bands at 480 and 483 cm^{-1} in the complexes.

In the mononuclear complex (**1**), (Fig. 2) the υ(O–H) band due to the O–H…O hydrogen bridges in the ligand is assigned at 3400 cm^{-1} and it appears as a very broad band. The IR spectrum of the BF_2^+ bridged complex (**2**) (Fig. 3) did not show this band. In the BF_2^+ bridged complex (**2**), bands at 1123 and 1035 cm^{-1} were observed for the B-O and B-F resonances,

respectively [32, 37, 38]. Their corresponding calculated wavenumbers appeared at 1142 and 1036 cm^{-1}. Details of the non-discussed modes are given as Supplementary Data in Tables S1-S3. The majority of the theoretical FT-IR values show good agreement with experimental values.

2.3. ^{1}H NMR Spectra

The theoretical ^{1}H NMR chemical shift values are given in Table 1. The atom positions are numbered in Fig. 1-3. The NMR spectra recognized that accurate predictions of molecular geometries are essential for reliable calculations of magnetic properties. Therefore the molecular structures of the title compounds were optimized before NMR calculations. Then, gauge-including atomic orbital (GIAO) ^{1}H NMR chemical shift calculations were carried out by using the DFT/B3LYP functional with the 6-31G(d) basis set. In the ^{1}H NMR spectrum of the ligand, the chemical shifts due to OH, NH and the phenyl ring hydrogens were observed at δ = 8.10, 7.03 and 7.15-7.68 ppm respectively. Their corresponding calculated chemical shifts appeared at 6.49 ppm for NH, at 7.30 and 5.75 ppm for OH and at 7.27-7.74 ppm for the phenyl ring. However, in the Cl bonded phenyl ring the ^{1}H NMR spectrum values decreased to the 6.50-7.09 ppm range. The ^{1}H NMR spectrum of complex (**1**) shows a singlet at 7.03 and 9.95 ppm assigned for hydrogen bonded NH and OH protons, respectively. These values were calculated as 5.54, 5.55 ppm for NH and as 13.04, 13.14 ppm for OH bonds. Chemical shifts for the hydrogen of the aromatics were assigned in the 7.05-7.59 region [15, 39, 40]. Additional signals at 7.81-8.43 ppm were caused by the coordinated pyridine molecule. They are theoretically found in the 6.53-7.57 ppm range for phenyl rings. Only the H14 and H47 atoms in the phenyl ring have the chemical shifts at 8.50 and 8.40 ppm, respectively. In the Cl bonded phenyl rings, ^{1}H NMR spectrum values decrease to 5.58-7.04 ppm range. In the ^{1}H NMR spectrum of complex (**2**), the deuterium exchangeable O–H…O bridged protons

belonging to the H-bonded dioxime complex were BF_2^+ bridged derivatives. The other chemical shifts in this complex, which belong to aromatic, aliphatic and NH protons, were very similar to this hydrogen-bonded Co(III) complex. In the ^{1}H NMR spectrum of the diamagnetic Co(III) complex, the singlet observed at δ=7.03 ppm can be assigned to the NH signal and signals at 7.91-8.71 ppm were caused by the coordinated pyridine molecule. The theoretical ^{1}H chemical shifts due to NH were found as 6.01 and 5.31 ppm. The ^{1}H NMR data of the complex support the proposed structure and are in good agreement with those of known oxime complexes [39-41].

2.4. ^{13}C NMR Spectra

The theoretical ^{13}C NMR chemical shift values are given in Table 2. Gauge-including atomic orbital (GIAO) ^{13}C NMR chemical shift calculations were carried out by using the DFT/B3LYP functional with the 6-31G(d) basis set. The atom positions are numbered in Fig. 1-3. ^{13}C values have been assigned for only a few organocobaloximes in the literature [17-20]. ^{13}C NMR spectra of complexes in the literature show some general trends that are described below. The ^{1}H and ^{13}C resonances of pyridine in complexes on coordination to the cobaloxime moiety shift downfield and this coordination shift (Δδ = δ complex - δ free Py) follows the order $\Delta\delta^{13}C\ Py_\gamma \geq \Delta\delta^{13}C\ Py_\beta > \Delta\delta^{13}C\ Py_\alpha$. The same order follows based on the ^{1}H NMR values. This coordination shift can be taken as a measure of the *trans* influence of the axial alkyl ligand.

The δ (C=N) is known to be sensitive to any change in the axial or equatorial environment in cobaloximes. C=N and Py_α resonances occur very close to each other. Theoretical values compared with literature values, similar trends were found to be.

2.5. Thermal Analyses

The thermal data of the complexes are given in Table 3. The TG/DTG diagrams of two complexes are given in Figs. 4 and 5. Thermochemical studies on cobalt complexes have been the focus of recent work. Brown *et al.* suggested that the first step involves the loss of the bottom axial base ligand. For the next stage, they propose the loss of the top axial ligand. Finally the complex, now bereft of both axial ligands, undergoes decomposition to form products, the nature of which was unreported [42]. Our results show that for the complexes, the above three transitions are not clearly separable, and the process of losing axial ligands is accompanied by the rupture of the equatorial dioxime ligand.

We can see from Fig. 4 that the thermal decomposition of complex (**1**) appears as a results of the loss of the axial pyridine ligand, benzyl group, biphenyl, and p-chloroaniline (temperature range 42–611 ºC, weight loss exp. 76.80 %; calc. 76.30). The complex shows residues not conforming to the corresponding metallic residue, such as metal oxide or metallic cobalt, even at 900ºC, indicate that the decomposition of the organic moiety remains incomplete even at this temperature.

Fig. 5 illustrates the thermal decomposition of the BF_2^+ bridged cobalt complex (**2**) which shows the loss of one axial pyridine ligand, a benzyl, two BF_2, two biphenyl and two p-chloroaniline (temperature range 19–892ºC, exp. 80.80 %; calc. 79.00 %). The decomposition of the organic moiety remains incomplete even at 900ºC.

2.6. Electrochemical Studies

The electrochemical properties of the ligand and its metal complexes were investigated in DMF containing 0.1 M TBAP as a supporting electrode by cyclic voltammetry (CV). All the measurements were carried out in $1x10^{-3}$ M solutions of the free ligand and its complexes at room temperature. For all CV measurements of the compounds at different scan rates in the range of 50-500 mVs^{-1}, the Epa values appear to depend only slightly on the scan rate (Fig. 6).

Furthermore, in all cases, a linear relationship between the cathodic peak current (ipa) and the square root of the scan rate was observed. This implies that these electrochemical processes are mainly diffusion-controlled.

The cyclic voltammogram of the ligand in DMF strongly shows one anodic wave in the positive range (+1.25 V) which can be attributed to the redox behavior (Fig. 7). The anodic peak current increases with increasing concentration of the ligand. This anodic wave, which is seen in the CVs for all metal complexes, is presumed to be ligand based oxidation.

The voltammograms of the metal complexes, in addition to the ligand peak, also have oxidation peaks. The representative voltammograms of complex (**1**) compared with the CV of the ligand is shown in Fig. 8. The obtained oxidation peak of the complex at the positive potential side indicated that the processes take place on the metal center of the complex.

2.6. Catalase-like Activity

Catalase enzymes are present in most aerobic forms of life and are responsible for the decomposition of hydrogen peroxide to molecular oxygen and water. Biomimetic compounds may help providing valuable insights into the mechanisms of these enzymes. Indeed, comparison of the activity of structurally characterized complexes can help delineating the functional roles of the ligands and that play a key function in H_2O_2 disproportionation. Several families of iron and manganese based catalysts are described [43-45], but the present study is focused on catalase like activity of the cobaloxime derivatives.

The catalase mimetic properties of the ligand and its complexes (**1** and **2**) in the presence of the base imidazole were investigated by measuring the volume of evolved oxygen during the course of the reaction. None of the compounds on their own exhibited catalytic activity. The imidazole base by itself causes only a very slight disproportionation of peroxide and that this reaction is greatly enhanced when the complexes are included in the reaction

mixture. Such an enhancement in the presence of added base has also been reported by other researchers [46-48].

The results from these reactions are summarized in Table 4 and Fig. 9. Table 4 shows the rate of evolution of oxygen from the respective reactions for the complexes over the first 15 min. All the complexes show activity for the catalytic decomposition of H_2O_2 in the presence of imidazole. Examination of Table 4 shows that, over the first minute, complex **2** appears to be the most efficient catalyst with 69 molecules of peroxide disproportionated by one molecule of the complex. The ligand appears to be the least efficient catalyst over the first minute with one molecule of the compound knocking down just 32 molecules of the peroxide. A comparison of the total number of molecules of H_2O_2 disproportionated by one molecule of the complex shows that complex **2** is the most effective catalyst with 173 molecules. The time course of the O_2 evolution is shown in Fig. 9. The H_2O_2 disproportionate efficiency of the complexes in the presence of imidazole, according to the total number of molecules of H_2O_2 disproportionated by one molecule, follows the order **2** > **1** > H_2L. In the absence of a heterocyclic base, the compounds decompose hydrogen peroxide slowly but the decomposition of H_2O_2 is enhanced in the presence of a heterocyclic base such as imidazole because of its strong π-donating ability [49]. On the other hand, heterocyclic bases themselves cause only a very slight disproportionation of the peroxide. As a result of catalase-like activity, the present complex (**2**) was found to have higher disproportionation efficiency when compared to other synthesized compounds.

2.7. Description of the Crystal Structure

Because of unsuccessful X-ray diffraction, the theoretical and recent literature data were used to clarify the geometric properties of the title molecules. The lowest energy structures found after an automatic conformational search were optimized with the DFT/6-31G(d) basis

set. The optimized structures and their atomic numbering are shown in Figs. 1-3. Because the structures have lots of atoms, the selected bond lengths, bond angles and dihedral angles are given as Supplementary Data in Table S4.

In the dioxime ligand, the phenyl rings are nearly planar and the angle between the two phenyl ring planes is found as 36.94°. The Cl-phenyl bond distance is 1.76 Å and the N-O distances are 1.37 and 1.42 Å.

In the complexes, the cobalt atom is linked to four nitrogen atoms belonging to the equatorial plane. The Co-atom displays an approximately octahedral coordination. The pyridine ring is practically planar and nearly perpendicular to the equatorial plane (Py-Co-N angles varying between 89.56-90.40° and 89.22-92.92° for complex (**1**) and complex (**2**), respectively). This is in agreement with the literature [50]. In complex (**2**), the angles are varied over a wide range. This can be explained by the two hydrogen bonds between the fluorine and pyridine hydrogen atoms. The Co-N_{ax} distance was 2.085 Å for the mononuclear complex (**1**) and 2.159 Å for the BF_2^+ bridged complex (**2**). It is reported in the 1.966 - 2.086 Å range for cobaloxime complexes in the literature [50-56]. The distance between Co and the axial pyridine is reported in the 1.945 - 2.066 Å range [51-56]. It was calculated as 2.022 and 2.046 Å for complexes (**1**) and (**2**), respectively. The axial angle between C-Co-N was found as 175.95° and 177.63° for complex (**1**) and (**2**), respectively. It is reported in previous studies at between 176.52-179.01 [51,54-56]. The Co-C-Ph angle was found as 113.63° and 119.92° for complexes (**1**) and (**2**), respectively.

3. Conclusion

In this work, new organocobaloxime derivatives of the types $[Co(HL)_2(Bz)Py]$ and $[CoL_2(Bz)PyB_2F_4]$ [H_2L = 4-(4-chlorophenylamino)biphenylglyoxime; Bz = Benzyl; Py = Pyridine] were synthesized and characterized by elemental analysis, ICP-OES, molar

conductance, FT-IR, ^{1}H NMR and magnetic susceptibility measurements. We also calculated the geometric parameters, vibrational frequencies and (^{13}C and ^{1}H) NMR spectra of the title molecules by using the DFT/B3LYP method with the standard 6-31G(d) basis set. The experimental and theoretical chemical shift results are generally in good agreement. The geometrical parameters are in agreement with previous experimental studies. The spectral and magnetic susceptibility data conform to the octahedral geometry expected for the complexes (Figs. 2, 3). There was not much variation in the magnetic properties, metal: ligand ratio and geometry of these complexes due to the replacement of BF_2 groups by the bridging protons of the dioxime complexes. The conductance data indicate that these complexes are non-electrolytes. The thermal analyses of the complexes show that these complexes thermally decompose and the organic moiety remains incomplete even at 900 ºC. Moreover, the catalytic activities of the complexes for the disproportionation of hydrogen peroxide were also investigated in the presence of imidazole. The catalytic results indicated that complex (**2**) has good catalase activity.

4. Experimental

4.1. Materials

All chemicals used in this work were of reagent grade and were used without further purification. 4-Biphenylchloroglyoxime was prepared according to Karipcin et al. [31].

4.2. Physical Measurements

The ^{1}H NMR spectra were obtained with a Bruker AVANCE instrument in DMSO-d_6 or $CDCl_3$, operating at 400 MHz. Proton chemical shifts δ are reported in part per million (ppm) relative to an internal standard of TMS. Elemental analyses and metal contents were performed by using a LECO 932 CHNS analyzer and a Perkin Elmer Optima 5300 DV ICP-OES spectrometer. IR spectra were recorded as KBr pellets using a Shimadzu IRPrestige-21

FT-IR spectrophotometer. Melting points were determined using an Electrothermal model IA 9100. The molar conductance was determined with an Optic Ivymen System conductivity meter. The magnetic susceptibilities of the prepared solid complexes were determined at room temperature using a Sherwood Scientific Magnetic Susceptibility Balance (Model MX1). Thermogravimetric analyses were carried out on a Perkin Elmer Diamond TGA thermal analyzer. The experiments were carried out in dynamic nitrogen atmosphere (20 mL min^{-1}) with a heating rate of 10ºC min^{-1} in the temperature range 20-900ºC.

4.3. Synthesis

4.3.1. Synthesis of the ligand {4-(4-Chlorophenylamino)biphenylglyoxime} (H_2L, $[C_{20}H_{16}N_3O_2Cl]$):

The ligand was prepared according to Karipcin *et al.*[31]. It was obtained by the reaction of 4-chloroaniline, (0.281 g, 2.2 mmol) with 4-biphenylchloroglyoxime (2 mmol, 0.55 g) in the presence triethylamine (309 µL, 2.2 mmol). The 4-chloroaniline and triethylamine dissolved in 10 mL methanol were added dropwise to a suspension of 4-biphenylchloroglyoxime in 50 mL methanol over 15 min. The mixture was stirred for a further 5-6 h, then diluted with 100 mL water. The resulting precipitate was filtered and then recrystallized from ethanol-water (1:4). The product was filtered, washed with water and dried.

Yellow, mp. 105°C, was isolated in 90% yield; IR (KBr disc. ν, cm^{-1}): 3367(N-H), 3212(O-H), 3030(C-$H_{(arom)}$), 2830(C-$H_{(aliph)}$), 1596,1635(C=N), 1493(C=C), 1092 (N-O); ^{1}H-NMR (δ, ppm): 8.10 s(2H, O-H…H), 7.15-7.68 m(13H, Ar-H), 7.03 s(1H, NH); molar conductivity (Λm): 10 $\Omega^{-1}cm^2mol^{-1}$; elemental analyses for $C_{20}H_{16}N_3O_2Cl$, Anal. Calcd.(%): C, 65.66; H, 4.38; N, 11,49, Found (%):C, 66.17; H, 4.59; N, 11.15 **[**30].

4.3.2. Synthesis of mononuclear complex, $[Co(HL)_2(Bz)Py]$ (1)

$CoCl_2.6H_2O$ (0.95 g, 4 mmol) and H_2L (2.93 g, 8 mmol) were stirred in methanol (35 mL), and dry nitrogen was passed through the mixture for 0.5 h. An aqueous solution of sodium hydroxide (0.32 g, 8 mmol, 2 mL) was added to the mixture, followed by pyridine (323 μL, 4 mmol). The mixture was cooled to 0°C and an aqueous solution of sodium borohydride (0.38 g, 10 mmol, 2 mL) was added. After 10 min. benzyl bromide (476 μL, 4 mmol in 2 mL of diethyl ether) was added dropwise to the reaction mixture. The reaction mixture was stirred for 5 h in nitrogen atmosphere and in the dark. Then the mixture was poured into 100 mL of ice-cold water containing a few drops of pyridine. The precipitate was filtered, washed with water and dried over P_2O_5.

Brown, mp. 289°C, was isolated in 92% yield; IR (KBr disc. ν, cm^{-1}): 3432 (N-H), 3400(O-H), 3056(C-$H_{(arom)}$), 2929(C-$H_{(aliph)}$), 1575,1590 (C=N), 1490(C=C), 1091(N-O), 498(Co-N); ^{1}H-NMR (δ, ppm): 9.95 s(2H, O-H…H), 8.43 d(αH-Py, 2H), 8.05 t(γH-Py, 1H), 7.81 t(βH-Py, 2H), 7.59-7.05 m(31H, Ar-H), 7.03 s(2H, NH), 2.85 s(2H, Bz); molar conductivity (Λm): 20 $\Omega^{-1}cm^2mol^{-1}$; diamagnetic; elemental analyses for $C_{52}H_{42}N_7O_4CoCl_2$, Anal. Calcd.(%): C, 65.14; H, 4.38; N,10.23,Co, 6.16, Found (%):C, 65.35;H, 4.19; N, 10.36; Co, 6.46 .

4.3.3. Synthesis of BF_2^+ bridged complex, $[Co(L)_2(Bz)PyB_2F_4]$ (2)

It was prepared by modifying the reported method [57]. A large excess of $C_2H_6OBF_3$ (280 μL, 3 mmol) was added to $[Co(HL)_2(Bz)Py]$ (0.480 g, 0.5 mmol) that was sealed in a flask under N_2. After the suspension was stirred for 5 min, 100 mL ACN and Et_3N (0.5 mL in 20 mL ACN) were added in succession. The suspension, sonicated for 10 min to break up large particles, was stirred overnight in the dark and in N_2. Then the solution was allowed to stand at -18°C overnight. After evaporation most of ACN under a reduced pressure and was added excess of isopropyl alcohol. The precipitate was filtered and dried over P_2O_5. Black, mp. 300°C, was isolated in 35% yield; IR (KBr disc. ν, cm^{-1}): 3446(N-H), 3057(C-$H_{(arom)}$),

2930(C-$H_{(aliph)}$), 1592(C=N), 1490(C=C), 1011(N-O), 515(Co-N), 1084(B-O), 1035(B-F); ^{1}H-NMR (δ, ppm): 8.71 s(2H, O-H…H), 7.71-7.11 m(36H, Ar-H), 7.03 s(2H, NH), 2.80 s(2H, Bz); molar conductivity (Λm): 30 $\Omega^{-1}cm^2mol^{-1}$; diamagnetic; elemental analyses for $C_{52}H_{40}N_7O_4B_2F_4CoCl_2$, Anal. Calcd.(%): C, 59.23; H, 3.82; N, 9.30, Co, 5.59, B, 2.05, Found (%):C, 59.46; H, 3.84; N, 9.20; Co, 5.82, B, 2.17.

4.4. Electrochemical studies

All electrochemical experiments were performed using Autolab PGSTAT 302 N (Eco Chemie, the Netherlands) Potentiostat/Galvanostat driven by the general purpose Electrochemical System data processing software (GPES, software version 4.9). A conventional three-electrode system was used. The working electrode was a platinum electrode of 2 mm diameter. The reference electrode was Ag/Ag+ (0.01 M) in nonaqueous media, and the counter electrode was a Pt wire. All solutions were purged with nitrogen steam for 20 min before measurement and the working electrode was polished before each experiment. Electrochemical experiments were performed in freshly distilled dry dimethylformamide (DMF) containing tetrabutylammonium perchlorate (TBAP) as a supporting electrolyte.

4.5. Studies on Catalase-like Function

The catalytic activity of the ligand and its complexes (**1** and **2**) towards the disproportionation of hydrogen peroxide was investigated by measuring the volume of evolved oxygen during the course of the reaction. Volumetric measurements of evolved dioxygen during the reactions of the compounds with H_2O_2 were carried out as follows: A 50 mL three-necked round-bottom flask containing a solution of the complexes (0.005 mmol solid sample) in DMF (10 mL) was placed in a water bath (25°C). One of the necks was

connected to a burette and the others were stoppered by rubber septa. While the solution was being stirred, H_2O_2 (2.60 mmol, 0.150 mL) was injected through the rubber septum using a microsyringe. Volumes of evolved dioxygen were measured at 1 min time intervals. In cases where imidazole (50 mg) was added, this was introduced into the reaction vessel before the addition of H_2O_2 (in the absence of imidazole the complexes were either inactive or very weak catalysts for this reaction).

4.6. Computational details

In the present study, Spartan 10 software [58] was used for the conformational search by using a PM3 semi-empirical model. All other calculations were performed by using Gaussian 09 [59] software. The calculations were carried out by solving the Kohn–Sham equations within the DFT framework. We employed the generalized gradient approximations (GGA) using the functionals of Becke's three-parameter hybrid exchange functional [60] and the Lee–Yang–Parr (LYP) nonlocal correlation functional [61]. The 6-31G(d) basis set was employed for gas-phase geometry optimization and to compute the vibrational frequencies.

Optimized structural parameters were used for vibrational and isotropic chemical shift calculations. Calculations for the NMR chemical shifts (^{1}H and ^{13}C) were carried out by using mostly the gauge-invariant atomic orbital (GIAO) method [62, 63]. The calculations reported were performed in chloroform solution using the IEF-PCM model, rather than in the gas phase, in agreement with experimental chemical shifts obtained in chloroform solution. The ^{1}H and ^{13}C NMR chemical shifts were reported in ppm relative to tetramethylsilane (TMS). Because there was no imaginary frequency for the stationary points, the optimized structure was accepted as real minimum.

Acknowledgements

This work was supported by the Research Fund of Süleyman Demirel University, Project no: 1505-D-07 (Isparta/Turkey). We would also like to thank Prof. Dr. Emin SARIPINAR for Spartan 10 performed at Erciyes University, Kayseri, Turkey.

References

[1] L. Tschugaeff, Ueber ein neues, empfindliches reagens auf Nickel, Ber. Dtsch. Chem. Ges. 38 (1905**)** 2520-2522.

[2] A. Chakravorty, Structure chemistry of transition metal complexes of oximes, Coord. Chem. Rev. 13 (1974**)** 1-46.

[3] V.Y. Kukushkin, A.J.L. Pombeiro, Oxime and oximate metal complexes: unconventional synthesis and reactivity, Coord. Chem. Rev. 181 (1999**)** 147-175.

[4] P. Chaudhuri, Homo- and hetero-polymetallic exchange coupled metal-oximates, Coord. Chem. Rev. 243 (2003) 143-190.

[5] A.G. Smith, P.A. Tasker, D.J. White, The structures of phenolic oximes and their complexes. Coord. Chem. Rev. 241 (2003**)** 61-85.

[6] Z. Biyiklioglu, G. Dilber, H. Kantekin, The synthesis and characterization of a new (E,E)-dioxime and its mono and heterotrinuclear complexes containing dioxadithiadiaza-macrobicyclic moieties, Transit. Metal Chem. 31 (2006) 979-985.

[7] D.C. Hodgkin, J. Kamper, J. Lindsey, M. MacKay, J. Pickworth, J.H. Robertson, C.B. Shoemaker, J.G. White, R.J. Prosen, K.N. Trueblood, The structure of vitamin B_{12} I. An outline of the crystallographic investigation of vitamin B_{12}, Proc. Roy. Soc. 242 (1957) 228-263.

[8] K.H. Reddy, The chemistry of vitamin B_{12} and model compounds, Coordination Compounds in Biology, Resonance 16 (2011) 1273-1283.

[9] G.N. Schrauzer, R.J. Windgassen, Alkylcobaloximes and their relation to alkylcobalamins, J. Am. Chem. Soc. 88 (1966), 3738-3743.

[10] F. Asaro, R. Dreos, S. Geremia, G. Nardin, G. Pellizer, L. Randaccio, G. Tauzher, S. Vuano, Diphenylborylated derivatives of organocobaloximes and organorhodoximes: Synthesis, spectroscopic and structural characterization, J. Organomet. Chem. 548 (1997) 211-221.

[11] R. Dreos, A. Felluga, G. Nardin, R. Randaccio, P. Siega, G. Tauzher, A new organocobalt complex containing a Co-N-C three membered ring, Inorg. Chem. 40 (2001) 5541-5546.

[12] R. Dreos, G. Nardin, L. Randaccio, P. Siega, S. Scagliola, G. Tauzher, The effect of the steric bulk of the ligand on the species self-assembled from Co(III) bis(dioximates) and boronic acids, Eur. J. Inorg. Chem. (2004) 4266-4271.

[13] R. Dreos, P. Siega, S. Scagliola, L. Randaccio, G. Nardin, C. Tavagnacco, M. Bevilacqua, Synthesis, characterization and electrochemical properties of dinuclear complexes assembled from asymmetric Co^{III} bis(dioximates) and boronic acids, Eur. J. Inorg. Chem. (2005**)** 3936-3944.

[14] B.D. Gupta, V.V. Kanth, V. Singh, Organocobaloximes: Synthesis, oxygen insertion and kinetics, J. Organomet. Chem. 570 (1998) 1-7.

[15] B.D. Gupta, K. Qanungo, Organobridged dicobaloximes: Synthesis and NMR correlation, J. Organomet. Chem. 534 (1997**)** 213-220.

[16] B.D. Gupta, K. Qanungo, Pyrazine bridged organodicobaloximes: A convenient one pot synthesis and cis influence studies, J. Organomet. Chem. 557 (1998) 243-249.

[17] B.D. Gupta, K. Qanungo, A study of cis influence in alkyl cobaloximes, J. Organomet. Chem. 543 (1997) 125-134.

[18] B.D. Gupta, K. Qanungo, R. Yamuna, A. Pandey, U. Tewari, V. Vijaikanth, V. Singh, T. Barclay, W. Cordes, Synthesis, characterization and cis-trans influence in cobaloximes with nioxime, J. Organomet. Chem. 608 (2000) 106-114.

[19] B.D. Gupta, V. Singh, K. Qanungo, V. Vijaikanth, R. Yamuna, T. Barclay, W. Cordes, Organocobaloximes with mixed-dioxime equatorial ligands: a one-pot synthesis, J. Organomet. Chem. 602 (2000) 1-4.

[20] B.D. Gupta, V. Singh, R. Yamuna, T. Barclay, W. Cordes, Organocobaloximes with mixed dioxime equatorial ligands: A convenient one-pot synthesis. X-ray structures and *cis-t**rans* influence studies, Organometallics 22 (2003) 2670-2678.

[21] B.D. Gupta, R. Yamuna, V. Singh, U. Tiwari, T. Barclay, W. Cordes, Organocobaloximes with mixed dioxime equatorial ligands: a convenient one pot synthesis. X-ray crystal structures of $BnCo^{III}$(dmgH)(dpgH)Py and $BnCo^{III}$(chgH)(dpgH)Py, J. Organomet. Chem. 627 (2001) 80-92.

[22] K. Kumar, B.D. Gupta, Synthesis, characterization, CV, and X-ray structures of aryl cobaloximes, J. Organomet. Chem. 695 (2010), 2233-2239.

[23] Mandal, B.D. Gupta, Cobaloximes with dimesitylglyoxime: Synthesis, characterization, and spectral correlations with the related cobaloximes, Organometallic, 24 (2005) 1501-1510.

[24] N. Navanettha, P.A. Nagarjun, S. Satyanarayana, Study of the spectroscopic characteristics of methyl (ligand) cobaloximes and their antibacterial activity, J. Chem. Sci. 119 (2007**)** 29-34.

[25] G.N. Schrauzer, R.J. Windgassen, On hydroxyalkylcobaloximes and the mechanism of a cobamide-dependent diol dehydrase, J. Am. Chem. Soc. (1967) 143-147.

[26] Z. Xin, H. Deyan, L. Yizhi, C. Huilan, Structure and thermal decomposition studies on alkylcobaloxime B_{12} model compounds with 1,2-cyclohexanedion dioxime as equatorial ligand, Inorg. Chim. Acta. 359 (2006) 1121-1128.

[27] C. Rovira, K. Kunc, M. Parrinello, Protonation state of the equatorial ligands and dynamics of the OH center dot O units in a cobaloxime biomimetic, Inorg. Chem. 41 (2002) 4810-4814.

[28] N.M. Shauib, A.Z.A. Elassar, A. El-Dissouky, Synthesis and spectroscopic characterization of copper(II) complexes with the polydentate chelating ligand 4,4'-[1,4-phenylenedi(nitrilo)dipente-2-one, Spectrochim. Acta A 63 (2006**)** 714-722.

[29] F. Karipcin, B. Dede, S. Percin-Ozkorucuklu, E. Kabalcılar, Mn(II), Co(II) and Ni(II) complexes of 4-(2-thiazolylazo)resorcinol: Syntheses, characterization, catalase-like activity, thermal and electrochemical behavior, Dyes Pigments,84 (2010) 14-18.

[30] N. Sundaraganesan, S. Ilakiamani, H. Saleem, P.M. Wojciechowski, D. Michalska, Spectrochim. Acta A 61 (2005) 2995.

[31] F. Karipcin, F. Arabali, F., Karatas, Synthesis and characterization of 4-arylaminobiphenylglyoximes and their complexes, J. Chil. Chem. Soc. 51 (2006) 982–985.

[32] F. Karipcin, M. Erdem-Tuncmen, G. Baskale-Akdogan, B. Dede, Synthesis and characterization of some borylated (4-biphenyl)(N-arylamino)glyoxime complexes, Pol. J. Chem. 83 (2009) 525–535.

[33] N. Yamazaki, Y. Hohokabe, Studies on cobaloximes and investigation on their infrared and far-infrared spectra, Bull. Chem. Soc. Japan, 44 (1971) 63–69.

[34] K. Burger, I. Ruff, F. Ruff, Infrared and ultra-violet spectrophotometric study of the dimethylglyoxime complex of transition metals, J. Inorg. Nucl. Chem. 27 (1965) 179–190.

[35] K. Nakamato, Infrared spectra of inorganic and coordination compounds, Wiley, New York, 1963.

[36] M. Erdem-Tuncmen, F. Karipcin, Synthesis and characterization of new organocobaloxime derivatives with asymmetric dioxime ligands, J. Incl. Phenom. Macrocycl. Chem. 77 (2013) 95-104.

[37] F. Karipcin, S. Ilican, Y. Caglar, M. Caglar, B. Dede, Y. Sahin, Synthesis, structural and optical properties of novel borylated Cu(II) and Co(II) metal complexes of 4-benzylaminobiphenylglyoxime, J. Organomet. Chem. 692 (2007) 2473-2481.

[38] A. Bilgin, B. Ertem, F.D. Agın, Y. Gok, S. Karslıoglu, Synthesis, characterization and extraction studies of a new vicdioxime and its complexes containing bis(diazacrown ether) moieties, Polyhedron 25 (2006) 3165-3172.

[39] C. Lopez, S. Alvarez, M. Aguilo, X. Solans, M. Font-Altaba, Synthesis and structure of chloro(ligand)bis(diphenylglyoximato)cobalt(III) complexes, Inorg. Chim. Acta 127 (1987) 153-159.

[40] C. Lopez, S. Alvarez, X. Solans, M. Font-Bardia, The influence of equatorial bulky substituents on the properties of organometallic bis(dioximato)cobalt(III) compounds—structural comparison between trans-[Co(dpgh)$_2$(R)(L)] complexes [dpgh = diphenylglyoximato(-1)] and other B-12 models, Polyhedron 11 (1992) 1637-1646.

[41] P.J. Toscano, L. Lettko, E.J. Schermerhorn, J. Waechter, K. Shufon, S. Liu, E.V. Dikarev, J. Zubieta, Synthesis and characterization of diphenylglyoximato cobalt(III) complexes. The molecular structures of trans-bis(diphenylglyoximato)-(alkyl)(pyridine)cobalt(III), with alkyl = CH_2SiMe_3, $CH_2CMe_3$and CF_3, Polyhedron 22 (2003) 2809-2820.

[42] T.M. Brown, A.T. Dronsfield, A.S. Wilkinson, Thermochemical studies of benzyl cobaloximes: A decomposition pathway different from that reported for the alkyl analogues, Inorg. Chim. Acta 262 **(**1997) 97-101.

[43] T. Okuno, S. Ito, S. Ohba, Y. Nishida, mu-Oxo bridged diiron(III) complexes and hydrogen peroxide: oxygenation and catalase-like activities, Dalton Trans. (1997) 3547-3551.

[44] W. Sicking, H.G. Korth, G. Jansen, H. de Groot, R. Sustmann, Hydrogen peroxide decomposition by a non-heme iron(III) catalase mimic: A DFT study, Chem. Eur. J. 13 (2007) 4230-4245.

[45] S. Signorella, C. Hureau, Bioinspired functional mimics of the manganese catalases, Coord. Chem. Rev. 256 (2012) 1229-1245.

[46] B. Dede, I. Ozmen, F. Karipcin, M. Cengiz, Homo- and heteropolynuclear copper(II) complexes containing a new diimine-dioxime ligand and 1,10-phenanthroline: Synthesis, characterization, solvent-extraction studies, catalase-like functions and DNA cleavage abilities, Appl. Organomet. Chem. 23 (2009) 512-519.

[47] S. McCann, M. McCann, M.T. Casey, M. Jackman, M. Devereux, V. McKee, Syntheses and X-ray crystal structures of *cis*-$[Mn(bipy)_2Cl_2]\cdot 2H_2O\cdot EtOH$ and *cis*-$[Mn(phen)_2Cl_2]$ (bipy = 2,2'-bipyridine; phen = 1,10-phenanthroline); catalysts for the disproportionation of hydrogen peroxide, Inorg. Chim. Acta 279 (1998), 24-29.

[48] G. Fernandez, M. Corbella, M. Alfonso, H. Stoeckli-Evans, I. Castro, A comparative XAS and X-ray diffraction study of new binuclear Mn(III) complexes with catalase activity. Indirect effect of the counteranion on magnetic properties, Inorg. Chem. 43 (2004), 6684-6698.

[49] E.J. Larson, V.L. Pecoraro, Manganese Redox Enzymes, Wiley-VCH, New York, 1992.

[50] B.D. Gupta, U. Tiwari, T. Barclay, W. Cordes, Inorganic cobaloximes with mixed dioxime equatorial ligands: a convenient one pot synthesis and *cis* influence studies: X-ray crystal structures of N_3Co^{III}(dmgH)(dpgH)Py and N_3Co^{III}(chgH)(dpgH)Py, J. Organomet. Chem. 629 (2001) 83-92.

[51] A.D. Follett, K.A. McNabb, A.A. Peterson, J.D. Scanlon, C.J. Cramer, K. McNeill, Characterization of Co-C bonding in dichlorovinylcobaloxime complexes, Inorg. Chem. 46, (2007) 1645-1654.

[52] K. Kumar, B.D. Gupta, Synthesis, characterization and structure-property relationship studies of cobaloximes with dithienylglyoxime as the equatorial ligand, J. Organomet. Chem. 696 (2011) 3785-3791.

[53] J. Galinkina, E. Rusanov, C. Wagner, H. Schmidt, D. Strohl, S. Tobisch, D. Steinborn, Synthesis, characterization, and reactivity of (fluoroalkyl)- and (fluorocycloalkyl)cobaloximes: Molecular structure of a (2-fluorocyclohexyl)cobaloxime complex and hindered rotation of 2-fluorocycloalkyl ligands, Organometallics 22 (2003) 4873-4884.

[54] M. Bhuyan, M. Laskar, B. D. Gupta, Biphenyl-bridged dicobaloximes: Synthesis, NMR, CV, and X-Ray study, Organometallics 27 (2008) 594–601.

[55] K.M. McCauley, S.R. Wilson, W.A. van der Donk, Synthesis and characterization of chlorinated alkenylcobaloximes to probe the mechanism of vitamin B-12-catalyzed dechlorination of priority pollutants, Inorg. Chem. 41 (2002) 393-404.

[56] P.G. Jones, L. Yang, D. Steinborn, cis-1,2-Dichlorovinyl)bis(dimethylglyoximato-N,N')(pyridine-N)cobalt(III) chloroform solvate, $[Co(dmgH)_2(py)\text{-}(CCI{=}CHCl)]\cdot CHCl_3$ Acta Crystallogr. C 52 (1996) 2399-2402.

[57] S.J. Moore, A. Kutikov, R.J. Lachicotte, L.G. Marzilli, Methyl B-12 models containing unsubstituted imidazole as an axial ligand investigated by structural and NMR spectroscopic methods. Evidence that mu-imidazolato-bridged dimers are formed by base addition to some analogues with macrocyclic equatorial ligands incorporating BF_2. Inorg. Chem. 38 (1999) 768–776.

[58] SPARTAN, Version 10, Wavefunction, Inc. 2006.

[59] M.J. Frisch, G.W. Trucks, H.B. Schlegel, G.E. Scuseria, M.A. Robb, J.R. Cheeseman, G. Scalmani, V. Barone, B. Mennucci, G.A. Petersson, H. Nakatsuji, M. Caricato, X. Li, H.P. Hratchian, A.F. Izmaylov, J. Bloino, G. Zheng, J.L. Sonnenberg, M. Hada, M. Ehara, K.

Toyota, R. Fukuda, J. Hasegawa, M. Ishida, T. Nakajima, Y. Honda, O. Kitao, H. Nakai, T. Vreven, J.A. Montgomery Jr, J.E. Peralta, F. Ogliaro, M. Bearpark, J.J. Heyd, E. Brothers, K.N. Kudin, V.N. Staroverov, R. Kobayashi, J. Normand, K. Raghavachari, A. Rendell, J.C. Burant, S.S. Iyengar, J. Tomasi, M. Cossi, N. Rega, J.M. Millam, M. Klene, J.E. Knox, J.B. Cross, V. Bakken, C. Adamo, J. Jaramillo, R. Gomperts, R.E. Stratmann, O. Yazyev, A.J. Austin, R. Cammi, C. Pomelli, J.W. Ochterski, R.L. Martin, K. Morokuma, V.G. Zakrzewski, G.A. Voth, P. Salvador, J.J. Dannenberg, S. Dapprich, A.D. Daniels, Ö. Farkas, J.B. Foresman, J.V. Ortiz, J. Cioslowski, D.J. Fox, Gaussian 09, Revision B.01, Gaussian Inc., Wallingford, CT, 2009.

[60] A.D. Becke, Density-functional thermochemistry. 3. The role of exact exchange, J. Chem. Phys. 98 (1993) 5648-5652.

[61] C. Lee, W. Yang, R.G. Parr, Development of the Colle-Salvetti correlation-energy formula into a functional of the electron-density, Phys. Rev. B 37 (1988) 785-789.

[62] R. Ditchfield, Molecular orbital theory of magnetic shielding and magnetic susceptibility, J. Chem. Phys. 56 (1972) 5688-5691.

[63] K. Wolinski, J.F. Hinton, P. Pulay, Efficient implementation of the gauge-independent atomic orbital method for NMR chemical-shift calculations, J. Am. Chem. Soc. 112 (1990) 8251-8260.

FIGURE CAPTIONS

Figure 1. The 3D and 2D structure and atomic numbering of the ligand (for clarity, the hydrogen atoms are omitted)

Figure 2. The 3D and 2D structure and atomic numbering of the complex (**1**) (for clarity, the hydrogen atoms are omitted)

Figure 3. The 3D and 2D structure and atomic numbering of the BF_2^+ bridged complex (**2**) (for clarity, the hydrogen atoms are omitted)

Figure 4. TG/DTG diagram of complex **1** $[Co(HL)_2(Bz)Py]$

Figure 5. TG/DTG diagram of complex **2** $[Co(HL)_2(Bz)PyB_2F_4]$

Figure 6. Cyclic voltammograms of complex **1** in DMF solution (0.1 M TBAP) at different scan rates (mV/s^{-1})

Figure 7. Cyclic voltammogram of $1.0x10^{-3}$ M ligand (KADO) in DMF solution (0.1 M TBAP) at scan rate of 100 mVs^{-1} versus Ag/Ag^+ electrode

Figure 8. Cyclic voltammograms of $1.0x10^{-3}$M complex **1** (b) in DMF (0.1 M TBAP) as compared to the CV of ligand (a) at scan rate of 100 mVs^{-1} versus Ag/Ag^+ electrode

Figure 9. Time courses of dioxygen evolution in the disproportionation of H_2O_2 by the ligand and its complexes (**1** and **2**) in DMF. [compound] = 0.005 mmol, $[H_2O_2]$ = 2.60 mmol, 298 K

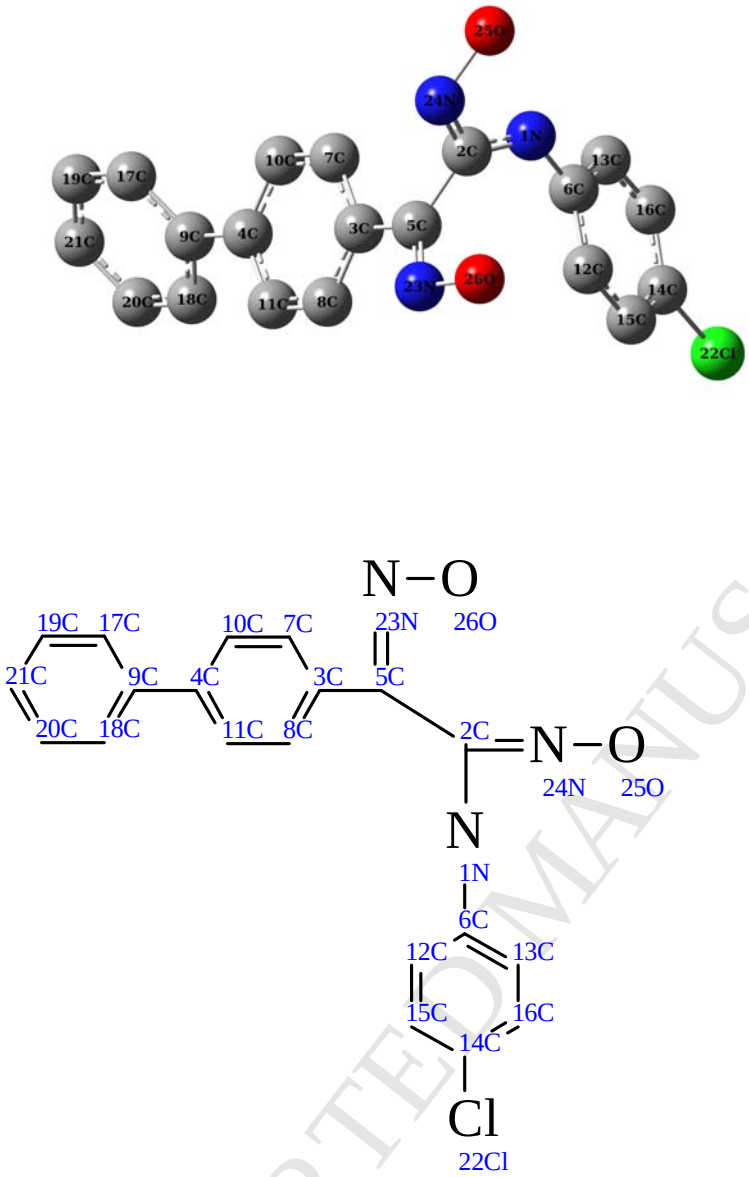

Figure 1. The 3D and 2D structure and atomic numbering of the ligand (for clarity, the hydrogen atoms are omitted)

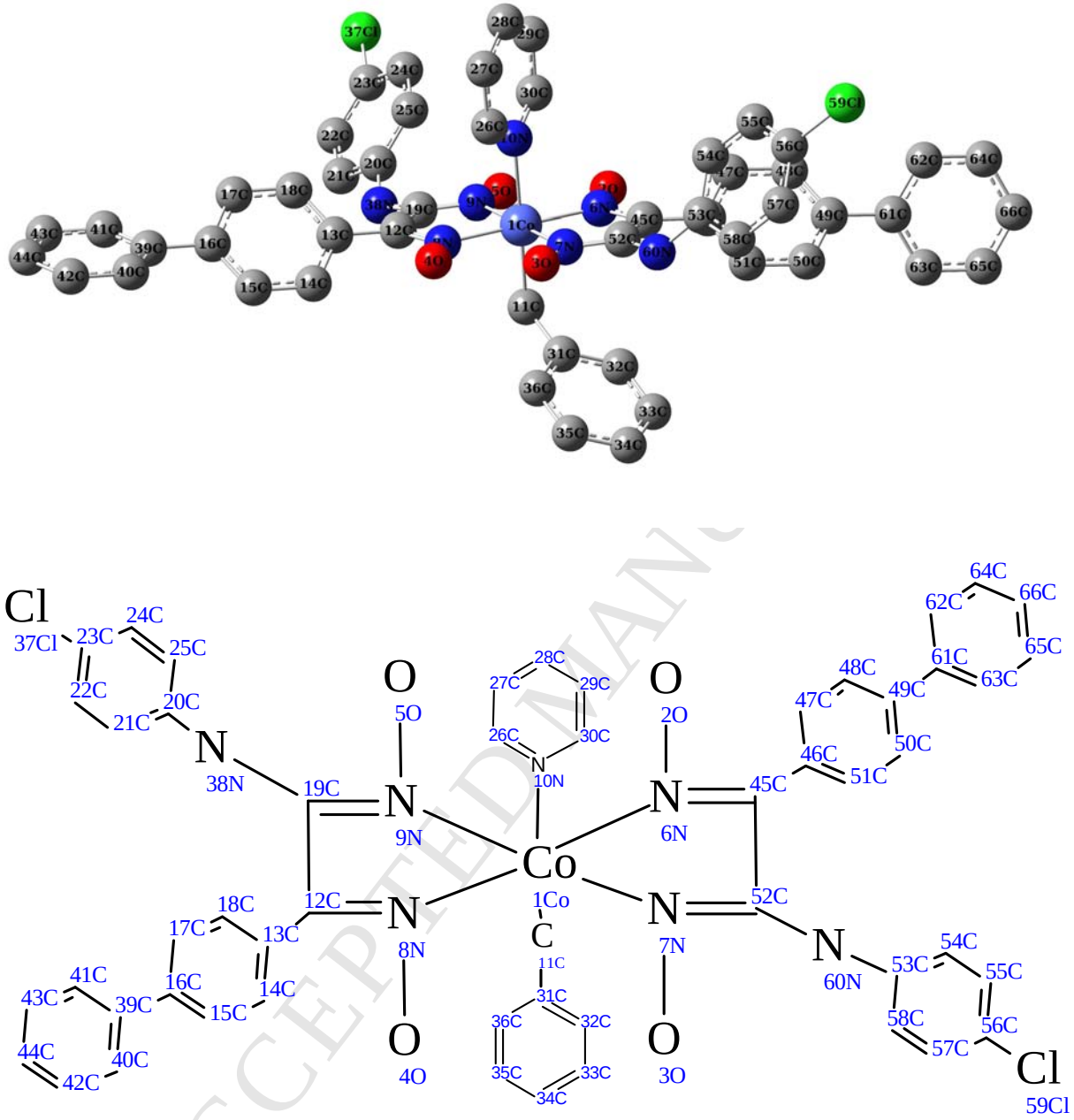

Figure 2. The 3D and 2D structure and atomic numbering of the complex (**1**) (for clarity, the hydrogen atoms are omitted)

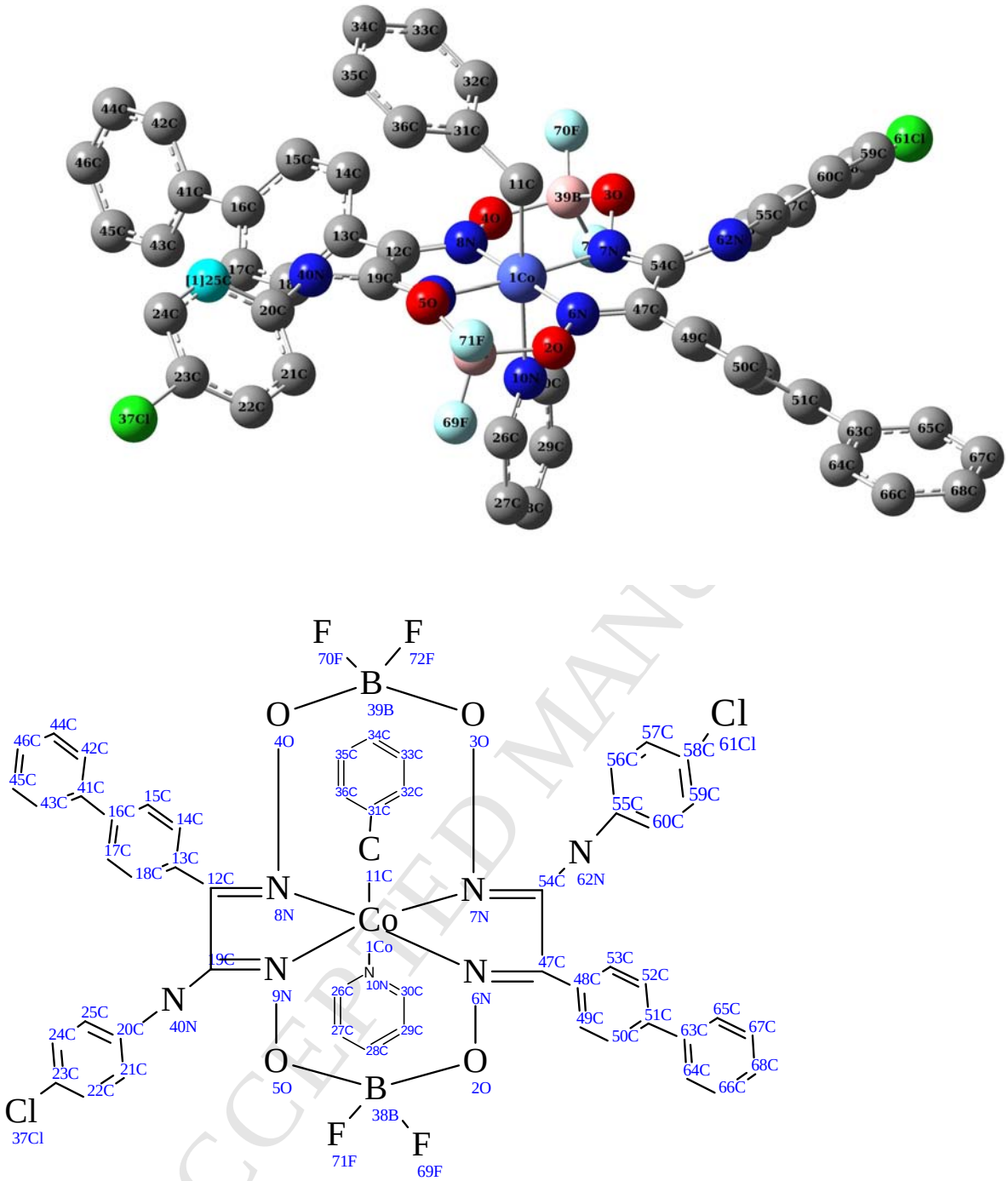

Figure 3. The 3D and 2D structure and atomic numbering of the BF_2^+ bridged complex (**2**) (for clarity, the hydrogen atoms are omitted)

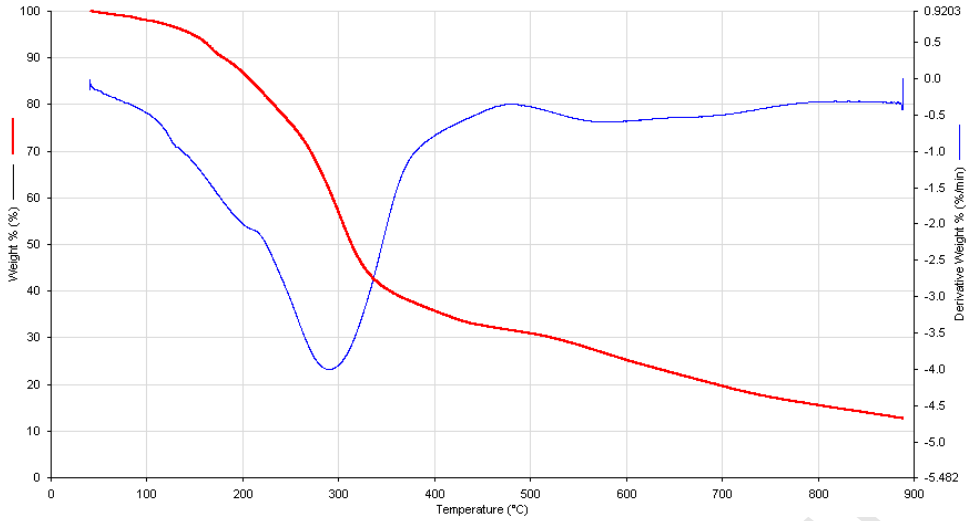

Figure 4. TG/DTG diagram of complex **1** $[Co(HL)_2(Bz)Py]$

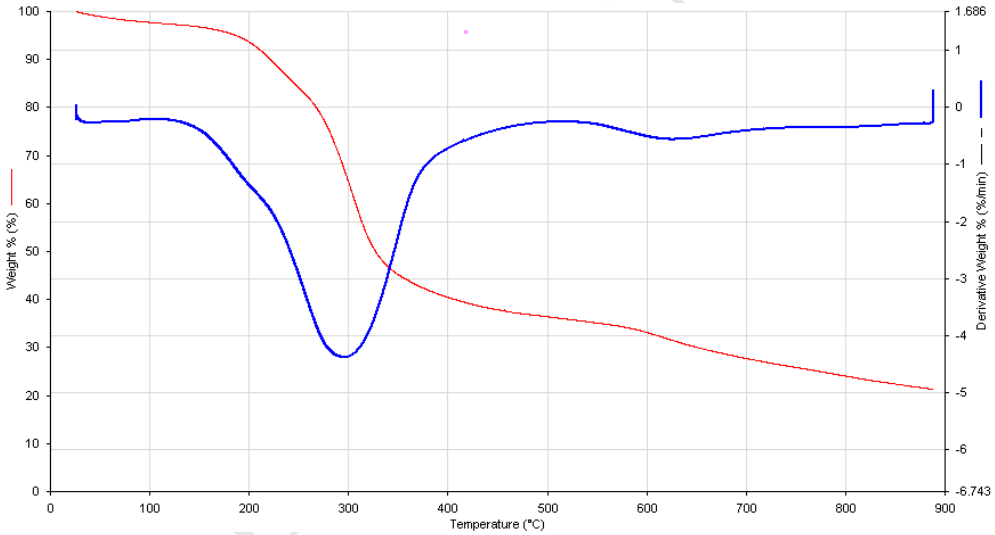

Figure 5. TG/DTG diagram of complex **2** $[Co(HL)_2(Bz)PyB_2F_4]$

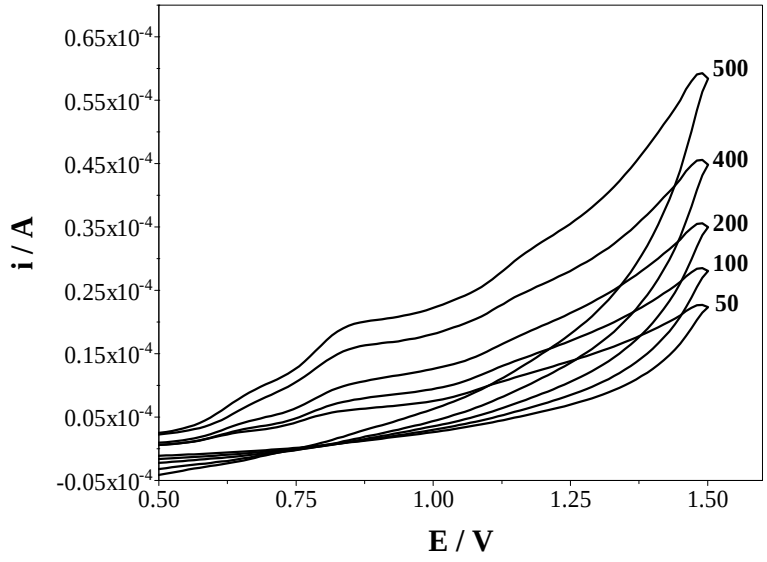

Figure 6. Cyclic voltammograms of complex **1** in DMF solution (0.1 M TBAP) at different scan rates (mV/s^{-1})

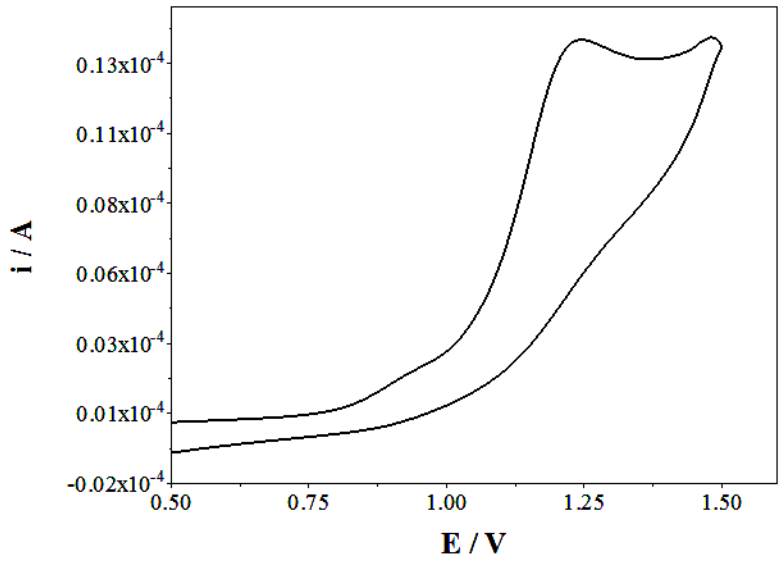

Figure 7. Cyclic voltammogram of $1.0x10^{-3}$ M ligand (KADO) in DMF solution (0.1 M TBAP) at scan rate of 100 mVs^{-1} versus Ag/Ag^{+} electrode

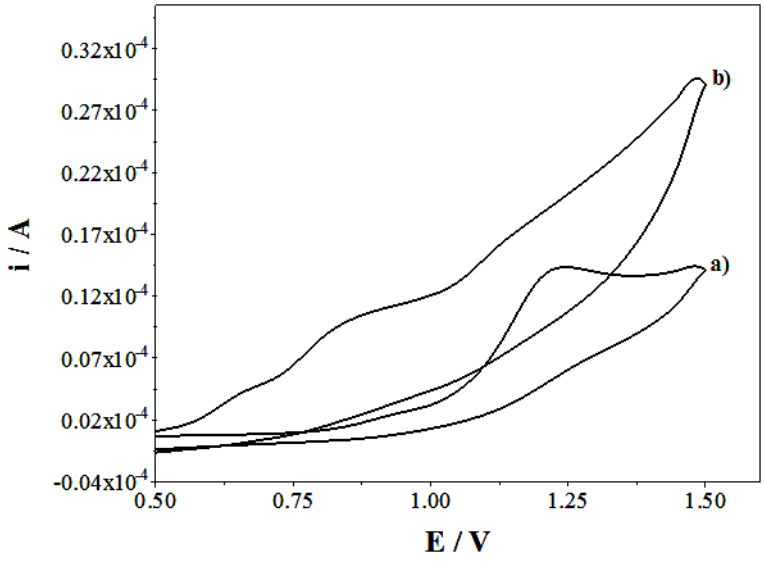

Figure 8. Cyclic voltammograms of $1.0x10^{-3}$M complex **1** (b) in DMF (0.1 M TBAP) as compared to the CV of ligand (a) at scan rate of 100 mVs^{-1} versus Ag/Ag^{+} electrode

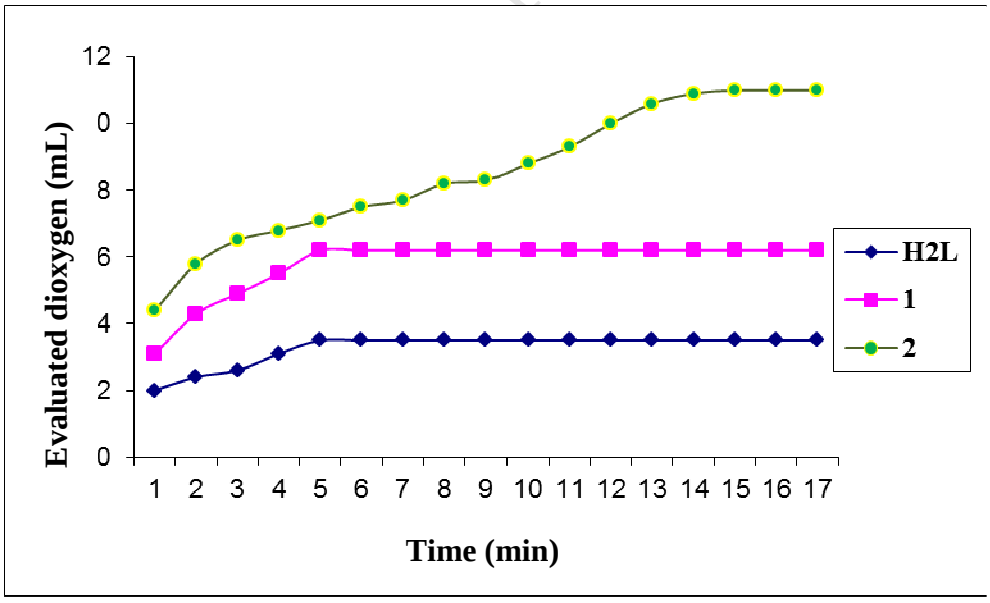

Figure 9. Time courses of dioxygen evolution in the disproportionation of H_2O_2 by the ligand and its complexes (**1** and **2**) in DMF. [compound] = 0.005 mmol, [H_2O_2] = 1.33 mmol, 298 K

Table 1. The predicted ^{1}H isotropic chemical shifts (with respect to TMS, all values in ppm) for presented molecules.

H_2L			**1**						**2**					
	Exp.	**Calc.**		**Exp.**	**Calc.**		**Exp.**	**Calc.**		**Exp.**	**Calc.**		**Exp.**	**Calc.**
H8	7.68	7.74	H3	9.95	13.14	H60	7.03	5.55	H26	8.71	9.69	H11B	2.80	2.72
H17	7.45	7.41	H5	9.95	13.04	H38	7.03	5.54	H30	8.71	9.55	H11A	2.80	2.37
H19	7.38	7.38	H30	8.43	9.12	H11A	2.48	2.30	H49	7.58	8.44	H40	7.03	5.31
H7	7.68	7.38	H26	8.43	8.87	H11B	2.48	2.22	H50	7.56	7.69	H27	7.91	7.30
H10	7.59	7.36	H14	7.59	8.50	H54	7.05	5.58	H28	8.10	7.67	H29	7.91	7.28
H20	7.38	7.35	H47	7.59	8.40	H44	7.47	7.34	H56	7.10	7.66	H17	7.56	7.27
H18	7.45	7.32	H28	7.90	7.80	H51	7.59	7.30	H14	7.58	7.65	H57	7.40	7.26
H26	8.10	7.30	H15	7.54	7.63	H36	7.45	7.27	H21	7.10	7.62	H22	7.40	7.25
H11	7.59	7.29	H29	7.81	7.61	H66	7.47	7.26	H64	7.49	7.60	H33	7.43	7.24
H21	7.32	7.27	H40	7.50	7.57	H27	7.81	7.25	H32	7.46	7.56	H59	7.40	7.05
H12	7.24	7.09	H42	7.50	7.45	H50	7.54	7.13	H66	7.49	7.49	H53	7.58	7.04
H15	7.15	6.92	H48	7.54	7.41	H35	7.46	7.12	H15	7.56	7.47	H36	7.46	7.01
H16	7.15	6.87	H63	7.50	7.41	H33	7.46	7.07	H44	7.49	7.44	H24	7.40	6.99
H13	7.24	6.50	H41	7.50	7.39	H24	7.41	7.04	H42	7.49	7.43	H34	7.43	6.91
H1	7.03	6.49	H43	7.50	7.39	H34	7.44	7.00	H52	7.56	7.42	H35	7.43	6.90
H25	8.10	5.75	H62	7.50	7.37	H22	7.41	6.98	H65	7.49	7.42	H18	7.58	6.78
			H64	7.50	7.37	H18	7.59	6.88	H67	7.49	7.42	H60	7.10	6.54
			H65	7.50	7.37	H32	7.45	6.75	H68	7.47	7.40	H25	7.10	6.38
			H17	7.54	7.34	H57	7.41	6.70	H45	7.49	7.38	H62	7.03	6.01
			H58	7.05	6.36	H25	7.05	6.64	H43	7.49	7.37			
			H55	7.41	6.26	H21	7.05	6.53	H46	7.47	7.32			

Table 2. The predicted ^{13}C isotropic chemical shifts (with respect to TMS, all values in ppm) for presented molecules.

H_2L		**1**				**2**			
	Calc.		**Calc.**		**Calc.**		**Calc.**		**Calc.**
5C	147.39	C45	140.08	C15	121.92	C47	146.62	C24	122.58
4C	138.17	C19	137.41	C18	121.71	C54	142.85	C18	122.51
2C	137.48	C16	137.02	C44	121.67	C19	141.73	C68	122.49
9C	135.14	C49	136.31	C4131	121.53	C31	140.91	C46	122.39
6C	130.88	C61	135.61	C40	121.52	C51	140.16	C15	121.98
14C	130.24	C39	134.84	C63	121.50	C16	139.70	C33	121.90
3C	126.29	C53	133.	C48	120.72	C41	134.50	C64	121.88
15C	123.56	C28	132.40	C33	120.64	C63	134.10	C42	121.80
16C	123.33	C20	131.29	C27	119.70	C28	131.99	C48	120.11
7C	122.96	C23	129.18	C29	119.60	C58	131.30	C13	119.70
20C	122.73	C56	128.70	C34	117.61	C23	130.99	C27	119.48
19C	122.67	C14	127.15	C25	115.59	C55	130.18	C29	119.42
11C	121.87	C47	125.45	C58	113.39	C20	130.02	C34	118.93
10C	121.75	C36	123.98	C21	113.28	C49	127.91	C56	118.06
21C	121.65	C46	123.97	C54	112.67	C14	127.65	C21	117.81
17C	121.46	C32	123.44	C11	40.13	C32	125.59	C60	114.12
18C	121.43	C57	123.32	C62	121.42	C36	124.33	C25	113.74
8C	120.96	C13	123.14	C17	121.36	C57	123.68	C11	43.76
12C	115.24	C51	122.95	C66	121.25	C22	123.68	C65	121.67
13C	115.07	C42	122.85	C35	121.05	C66	123.14	C43	121.64
		C43	122.75	C50	120.73	C53	122.95	C17	121.18
		C65	122.62	C26	144.37	C67	122.92	C35	120.84
		C55	122.58	C30	144.20	C44	122.89	C26	148.04
		C22	122.54	C31	143.60	C45	122.87	C30	147.72
		C64	122.49	C12	142.60	C50	122.65	C52	121.72
		C24	122.36	C52	141.60	C59	122.64	C12	147.37

Table 3. Thermoanalytical results (TG, DTG) of metal complexes

Compound	TG range (^oC)	DTG_{max} (^oC)	Estimated (%, calculated)	Assignment	Metallic residue
(1)	42-611	289	76.80 (76.30)	Loss of pyridine, benzyl, biphenyl and p-chloroaniline	Decomposition is in progress
	611-			Loss of other groups	
(2)	19-892	300	80.80 (79.00)	Loss of pyridine, benzyl, B_2F_4, biphenyl and p-chloroaniline	Decomposition is in progress
	892-			Loss of other groups	
	415-			Loss of other groups	

Table 4. Time course of oxygen evolution in molecules of H_2O_2 disproportionated by the ligand and complexes **1** and **2** with added imidazole (50 mg) at 25^{o}C

Time(min)	**H_2L**	**1**	**2**
1	32	49	69
2	38	68	91
3	41	77	102
4	49	87	107
5	55	98	112
6	55	98	118
7	55	98	121
8			129
9			131
10			139
11			147
12			158
13			167
14			172
15			173
16			173

Research highlights

· Two new organocobaloxime derivatives has been synthesized.

· The complexes characterized by the experimental methods like FT-IR, ^{1}H NMR spectra.

· The DFT calculations on the structure and vibrational spectra have been carried out.

· Calculated and experimental data are found to be in good agreement.

· Activities of the complexes for the disproportionation of H_2O_2 were investigated.

· The redox behaviors of the compounds have been investigated by cyclic voltammetry.

Table S1. The theoretical vibrational wavenumbers along with the irrelative intensities of the mononuclear complex of the dioxime ligand.

Mode	Freq.	Int.	Mode	Freq.	Int.	Mode	Freq.	Int.	Mode	Freq.	Int.
1	409	1.62	25	816	6.73	49	1134	2.83	73	1577	4.44
2	415	0.60	26	838	18.56	50	1174	0.03	74	1605	1.07
3	421	0.08	27	839	8.98	51	1195	5.65	75	1610	2.54
4	439	23.16	28	846	0.57	52	1196	0.47	76	1630	40.17
5	447	46.43	29	850	15.14	53	1204	22.88	77	1632	1.16
6	463	24.38	30	900	100.03	54	1233	55.69	78	1637	21.78
7	472	70.06	31	915	1.41	55	1268	79.13	79	1668	16.49
8	504	3.24	32	932	11.33	56	1291	1.71	80	1631	278.63
9	519	9.19	33	939	152.65	57	1294	1.79	81	3048	4.96
10	559	0.76	34	950	86.38	58	1304	46.36	82	3054	3.39
11	563	8.80	35	952	49.80	59	1314	7.27	83	3059	8.67
12	622	0.46	36	955	42.67	60	1321	5.70	84	3061	26.22
13	626	19.18	37	959	1.85	61	1331	0.16	85	3063	4.05
14	635	12.00	38	968	2.37	62	1338	54.87	86	3066	2.48
15	642	4.93	39	979	0.10	63	1348	1.80	87	3070	33.77
16	658	17.10	40	1000	0.19	64	1387	132.20	88	3077	24.36
17	681	11.88	41	1007	3.74	65	1393	97.20	89	3084	6.36
18	692	28.49	42	1013	15.65	66	1426	6.70	90	3084	3.69
19	701	18.94	43	1028	30.60	67	1433	26.21	91	3089	3.53
20	719	16.53	44	1047	43.96	68	1470	2.18	92	3091	3.26
21	738	22.76	45	1055	17.48	69	1491	4.10	93	3101	2.03
22	750	18.75	46	1094	49.77	70	1513	26.11	94	3442	53.35
23	770	13.50	47	1095	2.61	71	1524	219.84	95	3589	119.74
24	773	24.48	48	1126	5.32	72	1539	1.79	96	3623	114.73

Table S2. The theoretical vibrational wavenumbers along with their relative intensities of the trinuclear complex of the dioxime ligand.

Mode	Freq.	Int.	Mode	Freq.	Int.	Mode	Freq.	Int.	Mode	Freq.	Int.
1	400	39.27	42	643	4.49	83	902	47.33	124	1095	48.9
2	408	1.24	43	650	6.75	84	904	18.41	125	1095	4.11
3	409	0.09	44	654	1.14	85	915	1.59	126	1096	3.81
4	410	12.61	45	656	0.29	86	916	2.91	127	1115	48.9
5	415	0.31	46	685	8.15	87	925	0.27	128	1124	37.12
6	415	4.12	47	689	1.15	88	928	0.65	129	1126	5.46
7	416	0.59	48	700	7.16	89	929	0.83	130	1130	17.43
8	417	2.31	49	701	11.97	90	933	0.63	131	1134	7
9	417	1.58	50	702	17.3	91	950	0.47	132	1136	11.1
10	419	13.66	51	702	23.39	92	951	0.46	133	1144	2.92
11	420	14.45	52	702	54.9	93	953	2	134	1167	19.31
12	431	8.96	53	715	14.53	94	953	0.74	135	1167	2.91
13	436	14.92	54	721	37	95	957	0.88	136	1169	1.43
14	437	16.16	55	721	12.46	96	960	0.97	137	1173	0.13
15	443	6.18	56	731	8.1	97	961	1.93	138	1174	0.15
16	453	20.15	57	733	22.49	98	966	12.68	139	1181	230.82
17	457	65.82	58	761	28.2	99	970	0.2	140	1191	7.66
18	465	46.55	59	763	12.1	100	978	0.05	141	1193	11.97
19	480	125.72	60	765	53.29	101	980	0.07	142	1194	9.95
20	497	26.08	61	768	43.26	102	993	2.62	143	1196	1.27
21	498	14.23	62	786	16.13	103	997	0.3	144	1197	1.47
22	503	0.26	63	797	30.33	104	1000	2.01	145	1197	6.29
23	509	15.82	64	800	2.51	105	1000	1.46	146	1209	9.82
24	521	60.11	65	802	5.72	106	1002	3.41	147	1212	5.91
25	539	6.25	66	806	7.49	107	1006	12.91	148	1226	3.37
26	555	0.71	67	810	9.71	108	1007	9.64	149	1245	16.65
27	559	2.92	68	813	35.76	109	1011	22.19	150	1261	46.39
28	562	2.66	69	818	0.97	110	1011	24.39	151	1266	168.61
29	576	4.99	70	820	31.96	111	1020	12.26	152	1284	7.08
30	595	29.33	71	837	18.64	112	1026	0.21	153	1290	2.43
31	606	15.12	72	838	0.3	113	1027	1.28	154	1290	10.32
32	614	5.1	73	841	5.17	114	1035	2.35	155	1292	42.34
33	620	3.1	74	843	13.16	115	1037	1.29	156	1293	3.1
34	621	3.77	75	845	10.97	116	1040	2.54	157	1293	3.73
35	622	2.68	76	846	0.18	117	1044	17.27	158	1305	3.2
36	623	2.79	77	847	22.06	118	1053	0.28	159	1310	175.17
37	625	0.23	78	847	20.29	119	1054	1.32	160	1312	2.14
38	634	7.07	79	873	109.46	120	1075	4.73	161	1313	0.05
39	635	7.57	80	878	9.86	121	1083	15.33	162	1323	69.56
40	638	0.78	81	887	59.24	122	1089	3.95	163	1326	10.88
41	641	2.58	82	899	16.73	123	1094	98.09	164	1328	26.34

Table S2. (continued)

Mode	Freq.	Int.	Mode	Freq.	Int.	Mode	Freq.	Int.	Mode	Freq.	Int.
165	1333	1	188	1515	19.96	211	1637	17.2	234	3065	2.88
166	1333	6.76	189	1515	93.91	212	1638	9.47	235	3068	5.73
167	1338	4.43	190	1516	60.57	213	1669	18.18	236	3069	29.18
168	1344	0.28	191	1517	159.19	214	1680	20.11	237	3070	34.84
169	1347	3.56	192	1539	95.82	215	2640	24.81	238	3070	25.98
170	1347	6.68	193	1542	38.81	216	2678	4424.97	239	3074	15.74
171	1362	213.43	194	1549	349.23	217	2943	40.66	240	3077	29.65
172	1386	0.81	195	1572	1.24	218	3001	22.87	241	3078	30.13
173	1399	341.49	196	1575	0.64	219	3038	5.3	242	3080	4.87
174	1421	26.23	197	1591	504.68	220	3043	1.52	243	3081	6.41
175	1423	45.24	198	1602	28.96	221	3047	7.14	244	3085	3.81
176	1432	46.4	199	1606	0.97	222	3048	8.89	245	3087	3.09
177	1441	165.5	200	1607	4.33	223	3053	4.13	246	3090	5.13
178	1464	5.33	201	1610	6.79	224	3054	16.03	247	3091	4.8
179	1469	0.61	202	1610	1.88	225	3054	2.13	248	3091	3.19
180	1470	2.02	203	1614	7.03	226	3057	11.01	249	3092	10.59
181	1471	1.12	204	1615	79.49	227	3058	18.35	250	3094	2.63
182	1473	23.72	205	1629	24.11	228	3059	44.89	251	3101	15.24
183	1475	6.5	206	1629	15.66	229	3059	7.09	252	3109	1.68
184	1484	10.99	207	1630	31.4	230	3060	27.64	253	3110	2.35
185	1491	298.96	208	1632	1.74	231	3062	5.86	254	3112	4.09
186	1513	17.54	209	1633	5.43	232	3063	17.48	255	3408	39.05
187	1514	62.64	210	1637	10.4	233	3065	3.96	256	3441	76.07

Table S3. The theoretical vibrational wavenumbers along with their relative intensities of the mononuclear BF_2^+ bridged complex of the dioxime ligand.

Mode	Freq.	Int.	Mode	Freq.	Int.	Mode	Freq.	Int.	Mode	Freq.	Int.
1	401	4.96	42	632	8.38	83	850	20.05	124	1052	10.77
2	407	0.96	43	634	47.53	84	852	18.24	125	1052	4.56
3	408	0.91	44	638	0.42	85	855	0.68	126	1058	16.96
4	412	1.31	45	639	1.54	86	879	1036.64	127	1061	33.33
5	413	8.66	46	641	1.64	87	886	5.24	128	1080	4.1
6	414	1.07	47	649	39.16	88	918	0.89	129	1082	23.73
7	415	9.91	48	656	0.7	89	918	1.74	130	1093	3.74
8	416	1.98	49	657	2.67	90	919	12.05	131	1096	157.37
9	419	3.76	50	683	1.37	91	925	1.42	132	1096	4.85
10	421	1.73	51	687	0.37	92	926	2.69	133	1097	4.78
11	423	10.07	52	690	29.72	93	932	11.45	134	1097	3.82
12	429	3.51	53	694	2.22	94	946	59.1	135	1127	10.56
13	430	8.51	54	701	18.99	95	949	4.8	136	1130	74.38
14	437	3.27	55	702	19.85	96	954	4.03	137	1134	4.97
15	444	0.69	56	703	0.83	97	954	4.17	138	1135	33.47
16	469	27.15	57	704	24.07	98	955	0.86	139	1138	0.02
17	471	11	58	706	16.96	99	957	1.03	140	1142	208.39
18	483	108.41	59	707	27.98	100	960	3.27	141	1154	1.5
19	490	109.2	60	730	28.28	101	964	1.23	142	1166	110.6
20	494	18.21	61	732	17.88	102	969	0.23	143	1167	48.86
21	500	1.99	62	735	4.86	103	970	4.25	144	1168	12.13
22	504	17	63	742	1.38	104	979	2.12	145	1171	2.67
23	508	11.33	64	764	16.64	105	982	0.03	146	1175	0.03
24	515	56.95	65	767	36.47	106	982	16.84	147	1175	0.06
25	517	47.92	66	769	35.45	107	983	0.08	148	1188	4.66
26	525	8.97	67	770	17.3	108	997	0.46	149	1197	0.9
27	527	10.52	68	805	2.56	109	1000	1.77	150	1197	1
28	540	16.28	69	806	38.54	110	1000	3.86	151	1198	12.56
29	555	35.08	70	807	15.3	111	1006	12.75	152	1199	5.86
30	558	20.26	71	808	30.9	112	1006	11.66	153	1200	5.55
31	561	4.23	72	812	111.99	113	1007	2.54	154	1211	8.35
32	569	16.36	73	816	11.48	114	1009	0.44	155	1211	9.36
33	570	1.16	74	824	22.93	115	1011	26.96	156	1218	252.4
34	578	27.14	75	830	50.71	116	1012	5.16	157	1227	1.55
35	602	6.2	76	836	0.51	117	1015	6.31	158	1232	293.7
36	610	10.39	77	837	159.44	118	1027	85.5	159	1247	14.14
37	617	1.42	78	842	20.42	119	1028	9.8	160	1252	8.37
38	621	17.15	79	844	33.93	120	1032	63.18	161	1254	283.69
39	622	0.33	80	846	10.07	121	1036	450.65	162	1271	2.18
40	624	0.26	81	847	3.9	122	1040	34.95	163	1279	20.86
41	625	125.92	82	848	108.58	123	1050	25.08	164	1284	0.83

Table S3. (continued)

Mode	Freq.	Int.	Mode	Freq.	Int.	Mode	Freq.	Int.	Mode	Freq.	Int.
165	1289	8.94	190	1470	2.96	215	1628	5.22	240	3070	12.7
166	1290	24.88	191	1471	0.68	216	1632	9.46	241	3070	14.22
167	1293	3.5	192	1475	3.44	217	1632	5.37	242	3073	15.27
168	1293	4.41	193	1511	35.61	218	1636	30.76	243	3073	14.43
169	1301	3.76	194	1512	64.31	219	1637	41.14	244	3076	7.55
170	1304	37.99	195	1515	244.47	220	1639	28.86	245	3077	13.09
171	1315	0.04	196	1515	61.63	221	1643	518.5	246	3077	11.18
172	1316	0.06	197	1516	8.56	222	1647	293.71	247	3079	30.24
173	1326	1.45	198	1526	1.33	223	2969	24.95	248	3080	28.26
174	1327	13.65	199	1532	2.3	224	3033	12.14	249	3084	8.63
175	1334	10.61	200	1534	3.19	225	3040	2.44	250	3090	7.13
176	1335	0.52	201	1552	174.97	226	3049	12.15	251	3091	4
177	1335	21.78	202	1554	197.96	227	3050	6.99	252	3092	4.54
178	1347	20.58	203	1568	34.44	228	3050	7.67	253	3092	1.58
179	1347	1.88	204	1570	42	229	3052	10.03	254	3093	1.56
180	1348	1.08	205	1575	44.53	230	3052	9.87	255	3110	0.42
181	1355	122.81	206	1579	61.3	231	3056	1.46	256	3110	0.34
182	1356	51.12	207	1605	1.04	232	3056	1.05	257	3135	15.19
183	1398	1.71	208	1610	1.25	233	3060	16.43	258	3137	15.2
184	1426	28.17	209	1610	0.7	234	3061	16.11	259	3139	31.27
185	1426	28.9	210	1610	1.82	235	3061	24.04	260	3142	42.81
186	1432	36.86	211	1619	60.45	236	3065	13.99	261	3435	111.08
187	1432	28.02	212	1620	64.69	237	3065	12.5	262	3436	74.97
188	1469	32.69	213	1625	60.5	238	3066	6.5			
189	1470	2.18	214	1626	6.76	239	3068	23.42			

Table S4. Bond lengts, bond angles and dihedral angles of a) the mononuclear complex of the dioxime ligand b) the trinuclear complex of the dioxime ligand c) the mononuclear BF_2^+ bridged complex of the dioxime ligand.

(a)		**(b)**		**(c)**	
R(1,2)	1.37	R(1,10)	2.09	R(1,10)	2.16
R(1,6)	1.41	R(1,11)	2.02	R(1,11)	2.05
R(5,37)	1.29	R(1,6)	1.92	R(1,6)	1.88
R(2,5)	1.50	R(1,7)	1.89	R(2,38)	1.55
R(3,5)	1.48	R(2,6)	1.30	R(2,6)	1.33
R(2,24)	1.29	R(3,7)	1.38	R(23,37)	1.76
R(4,9)	1.48	R(12,19)	1.48	R(38,69)	1.40
R(23,26)	1.40	R(56,59)	1.76	R(38,71)	1.36
R(24,25)	1.43	R(19,38)	1.38	R(6,47)	1.31
R(14,22)	1.76	R(20,38)	1.41		
		R(16,39)	1.48	A(47,48,49)	121.72
A(2,5,3)	118.52			A(50,51,63)	121.21
A(1,2,24)	123.59	A(1,11,31)	119.48	A(6,2,38)	124.01
A(2,5,23)	126.84	A(1,8,4)	122.10	A(6,47,48)	125.43
A(2,1,6)	123.67	A(1,8,12)	115.93	A(1,11,31)	119.92
A(1,6,12)	122.29	A(8,12,13)	124.40	A(1,6,2)	125.08
A(1,2,5)	120.74	A(8,12,19)	112.17	A(1,6,47)	115.83
A(5,3,7)	120.78	A(12,19,38)	119.78	A(2,38,69)	105.63
		A(15,16,39)	121.30	A(2,38,71)	105.07
D(11,4,9,17)	142.97	A(19,38,20)	129.31		
D(8,3,5,2)	162.23			D(1,11,31,32)	-86.93
D(5,2,24,25)	175.91	D(15,16,39,40)	36.67	D(15,16,41,43)	143.02
D(1,2,5,3)	97.62	D(7,52,60,53)	-131.59	D(1,6,47,48)	-173.18
D(2,1,6,13)	-34.59	D(58,53,60,52)	-172.59	D(1,7,54,62)	-164.38